

OPTIMIZING SPECTRUM SENSING PERFORMANCE IN AERONAUTICAL- LDACS SYSTEMS THROUGH LOW-POWER CORRELATOR-BASED TECHNIQUES

Dr. A S Rathore¹ P Surendrababu²

¹Research Guide, Dept. of Electronics and Communication Engineering , Sri Satya Sai University of Technology and Medical Sciences, Sehore Bhopal-Indore Road, Madhya Pradesh, India

²Research Scholar , Dept. of Electronics and Communication Engineering, Sri Satya Sai University of Technology and Medical Sciences, Sehore Bhopal-Indore Road, Madhya Pradesh, India

Abstract

A disturbing measure of individuals is flying at this point. The most up to date research on European flight by Euro control demonstrates that how much range that is at present accessible will oblige the increment of air traffic. The L-band computerized aeronautical correspondence framework (LDACS) has drawn continuous interest as one of the ways of conveying air/ground (A/G) broadband correspondence. It is rapidly developing into the picked model for extreme execution. The global common flight association (ICAO) has found numerous 1 MHz void groups between adjoining distance estimating hardware (DME) signals for LDACS in view of different range estimation examinations. The possibility of dynamic range access (DSA), which requires the utilization of range detecting strategies to find the range holes made by DME clients, can be utilized to the LDACS to increment range effectiveness. The properties of DME beat signals are utilized to propose a versatile edge energy identification range detecting approach in this article.

Keywords: Aeronautical, LDACS Low-Power, Correlator, DME

1. INTRODUCTION

A disturbing measure of individuals is flying at this point. The freshest exploration on European flight by Euro control shows that how much range that is right now accessible will oblige the increment of air traffic. The L-band computerized aeronautical correspondence framework (LDACS) has drawn continuous interest as one of the ways of conveying air/ground (A/G) broadband correspondence. (D. Li, 2016.) It is rapidly advancing into the picked model for extreme execution. The global common flying association (ICAO) has found numerous 1 MHz void groups between adjoining distance estimating hardware (DME) signals for LDACS in view of different range estimation examinations. The possibility of dynamic range access (DSA), which requires the utilization of range detecting strategies to find the range holes made by DME clients, can be utilized to the LDACS to increment range productivity. The properties of DME beat signals are utilized to recommend a versatile limit energy discovery range detecting approach in this article. We propose an original L-band computerized aeronautical correspondence framework (LDACS) utilizing reconfigurable separated OFDM to address the developing requirement for range for aeronautical correspondence (Ref-OFDM). (E. Abd-Elaty, 2020.) To accomplish the fundamental nature of administration, the proposed

convention empowers handsets to change the transmission data transfer capacity across a wide reach progressively. High out-of-band constrictions additionally essentially works on the use of the accessible range. We give reenactment and intricacy examination discoveries for a scope of sensible channel circumstances to back up our cases.

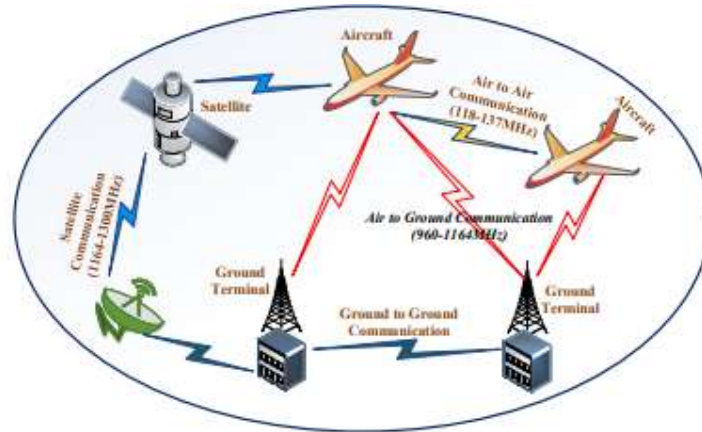


Figure 1: The future communication infrastructure (FCI) system has a number of communication linkages.

Conveyed on the 19 MHz VHF band during the 1990s (118-137 MHz). Thus, it is known as VHF Information Connection (VDL) and is much of the time used in current frameworks. As found in Fig. 1, aerial correspondence additionally utilizes the VHF recurrence. (Sebastian, 2019)The burdens of the VDL-based framework incorporate extreme blockage welcomed on by less correspondence lines and unfortunate information rates, which confine the scope of administrations that might be conveyed. L-band computerized aeronautical correspondence framework (pioneering range access based decorate strategy) was created in 2007 to empower A2GC in the L-band (960-1164MHz) (LDACS). It is guessed that it will actually want to offer a great many administrations, including telephone, information, and state of the art delay-delicate interactive media applications, by exploiting open recurrence groups between existing L-band clients. The LDACS prerequisites were finished in 2009, and the primary model has recently been shown off

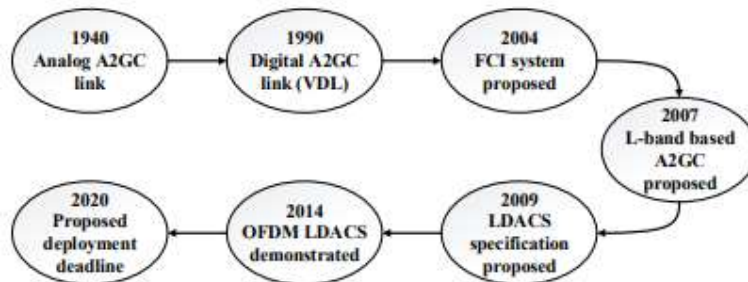


Figure 2: A2GC system progression in brief history.

The proposed LDACS is partitioned into two subsystems: 1) Symmetrical recurrence division multiplexing is the underpinning of the broadband multi-transporter framework known as LDACS1 (OFDM). It uses two advancements: 1) LDACS2: Narrowband single transporter framework in light of time division duplex method, which is indistinguishable from IEEE

802.16 norm, and 2) decorate approach between current distance estimation gear (DME) signals. (L. K. Mathew and A. P. Vinod, 2016) It utilizes a Gaussian least shift keying tweak technique and is tantamount to the Worldwide Framework for Versatile Correspondence (GSM). Because of its ability to deal with rapid deferral delicate mixed media administrations and interoperability with cell correspondence guidelines, LDACS1 has all the earmarks of being a predominant choice for the cutting edge A2GC framework the exploration depicted in this paper will hence focus on LDACS1, which we will allude to as LDACS from here on.

The range should be used actually assuming ATM quality is to be gotten to the next level. Strategies in view of mental radio (CR) have been created to increment correspondence limit and range effectiveness. (L. K. Mathew, 2019) The most utilized range detecting methods these days are energy location, cyclic fixed qualities discovery, and matching channel identification. A fast and effective way to deal with see the world while blind is utilizing energy recognition. While matched channel location just requires fractional data on the essential client, cyclic fixed highlights recognition might require some, like measurable property. There are additionally range detecting strategies in light of the wavelet change, signal trademark esteem, and other sign handling methods. (M. Mostafa, 2014) Additionally, comparative L-band range detecting procedures are utilized in the field of aeronautical correspondence, including the energy distinction technique low-power correlator strategy and cyclic prefix supported approach.

Besides, DME signals are identified through cognizance recognition and power identification the previous offers a relationship between's segments of the got signal and moved segments by using the rehashed idea of DME beat matches. However in light of the fact that OFDM and DME signals don't correspond the same way, the cycle is very difficult. (M. Sajatovic, 2009.) The last option utilizes a Gaussian-molded obstruction range and might be utilized with a decorate framework that utilizes LDACS. By the by, it isn't versatile and ignores the effect of the OFDM signal. (M. Schnell, 2014) The versatile limit energy location strategy for recognizing the DME signal was proposed in this exploration. The essential client signal is the (e DME signal, and the approved client signal is the OFDM signal. The DME signal, OFDM sign, and clamor are parts of the got signal.

2. REVIEW OF LITREATURE

While it was normal to anticipate variations in channel response due to grid deployment practices at different locations around the world, Francisco Canete et al. (2011) highlighted the special characteristics of the PLC channel with the observation that even in a specific network, the choice of the sockets to connect the transmitter and the receiver of the communications system strongly influenced the channel response. Both excessive attenuation over short distances and the appearance of notches at specific frequencies where the attenuation increases abruptly by up to 30 dB were noted as distortions. (M. Schnell U. E., 2009) Cortes et al. (2015)'s measurements revealed the variations in channel features across rural, semi-urban, and urban locations. The tests revealed that the semi-urban regions had the best performance, with 90% of the channels able to supply data rates more than 153 kbps, compared to urban areas where the comparable threshold data rate was 28 kbps.

Galli and Banwell (2004) established the feature of symmetry by asserting that, when driven from either side and given identical source and load impedances, the PLC channel, regardless of its topology, shows the same transfer function.

According to Zhu et al. (2013), modeling of PLC channels is difficult because of a variety of factors, including the harshness and diversity of power line networks and the challenges with measurement. In general, physical (or bottom-up) and parametric (or top-down) models of PLC channels may be distinguished. Based on the cable's specification, length, and branch placement, the physical models explain the electrical characteristics of the communications channel.

The Channel Transfer Function or Impulse Response is used by parametric models to characterize the communications channel (CTF). Moreover, deterministic and stochastic models are subdivided into the physical and parametric models (Tonello and Versolatto 2010; 2011a; 2011b). Whereas the stochastic models reflect a greater variety of channel realisations and are translated to a probability function, the deterministic models only represent one or a restricted number of particular channel realisations. (M. Schnell U. E., 2009.)

The power line components and loads are represented by ABCD parameters from equations (2.2) to (2.4) or S-parameters (Scattering parameters) in the physical deterministic models, and the channel transfer function is calculated (Bakhoun 2011). Esmailian et al. (2003) determined the transfer function of in-building power line channels using the transmission line theory. On the basis of experimental data, the real transfer functions were also derived. Measurements were made of the per-unit-length values for resistance R (/m), inductance L (H/m), conductance (S/m), and capacitance (F/m).

Based on Multi-conductor Transmission Line (MTL) theory, Sartenaer and Delogne (2006) provided a comprehensive technique for the deterministic modeling of the transfer function of the communications channel. (N. Neji, 2013.) The identification of propagation modes as a function of cable geometry was the first stage in this procedure, and in the second step, channel discontinuities such cable interconnections and terminations were taken into consideration. Canete et al. (2003) suggested a model based on the physical characteristics of the power lines that could be used for any network architecture as long as the approximate size and length of the cable, quantity of branch circuits, and kind of cables were known. A physical deterministic channel model for broadband communication on power lines was created by Barmada et al. in 2006. The two-port network-based channel model that was suggested used a scattering matrix. In order to verify the correctness of the MTL method, Galli and Banwell (2006) provided a study of measurement data. They also supported the usage of a physical deterministic model based on the MTL theory for both grounded and ungrounded power line channels. Also, it was asserted that the power line channel showed greater determinism than was previously thought. To evaluate the transfer function of a two-conductor power line system (one-phase conductor and the neutral conductor), Anatory et al. (2009a) suggested a deterministic communications model utilizing a generalized transmission line technique.

Transfer functions were calculated for two topologies: scattered branches along the main line section and branches concentrated at a single node. The model was expanded to a network with a tree topology and findings were found to be acceptable, demonstrating that the suggested model could be applied for any network architecture. This model was also expanded for multiconductor systems (Anatory et al. 2009b). Many criteria derived from accepted cabling procedures constitute the foundation of physical stochastic models. With the extra benefit of

supporting stochastic channel realisations, these models offer the same levels of accuracy as the deterministic model (Anastasiadou and Antonakopoulos 2005).

The most popular models are deterministic parametric models. To simulate and analyze the functioning of channels, these models draw on a database of observed characteristics such the channel transfer function. To reduce modelling errors, a sizable and varied database is necessary. The parametric stochastic models are based on actual data, such as the impulse response or the channel's transfer function, rather than necessarily on the physical phenomena of electromagnetic wave transmission (Meng et al. 2004)

3. THE SIGNAL CHARACTERISTIC

3.1. DME Signal

Radio route gear known as DME estimates the distance between an ethereal station and a ground station (GS) (AS). With this framework, there are 126 X channels and 126 Y channels, adding up to 252 possible channels. The ground reaction recurrence is 962-1213 MHz, while the airborne request recurrence is 1025-1150 MHz. The 1 MHz (e channel recurrence stretch. The construction of one DME beat pair and the gave boundaries are clarified in Figure 2. As can be seen from it, the half-width of the Gaussian-formed beats is 3.5 s, and the time between beat matches is 12 s.

This concentrate just examines the DME signal sent by one DME stage, despite the fact that the OFDM collector of LDACS might get a few DME signals from numerous DME stages. DME sends beat matches, which are comprised of sets of heartbeats with a time frame and have a Gaussian structure. A DME signal is a couple of heartbeats with a Gaussian structure that are numerically addressed by

$$b(t) = e^{-\epsilon/2t^2} + e^{-\epsilon/2(t-\Delta t)^2} \quad (1)$$

Where the transmission method of DME decides the time frame Gaussian-formed beat pair t, and the potential qualities are 12 and 36 seconds.

(1) Also gives the following model of the beat impedance sign of DME.

$$i(t) = \sum_{i=0}^{N_1-1} \sum_{u=0}^{N_u-1} A_i^{DME} b(t - t_{i,u}) e^{j2\pi f_{c,i}t} \quad (2)$$

N_1 signifies the amount of DME obstruction sources, I means the chronic number of a DME obstruction source, u signifies the chronic number of a DME beat pair, $N_{u,i}$ signifies the all out number of heartbeat matches delivered by the i th DME impedance source all through the perception period, $t_{i,u}$ indicates the moment at which the u th beat pair created by the i th DME impedance source initially shows up, and $t_{i,u}$ can be displayed as DME I addresses the pinnacle power of the beat signal sent by the i th impedance wellspring of DME, and $A_{DME I}$ addresses the pinnacle sufficiency of the beats. $f_{c,i}$ addresses the offset of the transporter recurrence of the sign communicated by the i th obstruction wellspring of DME. i,u addresses the underlying period of the transporter signal sent by the i th impedance wellspring of DME.

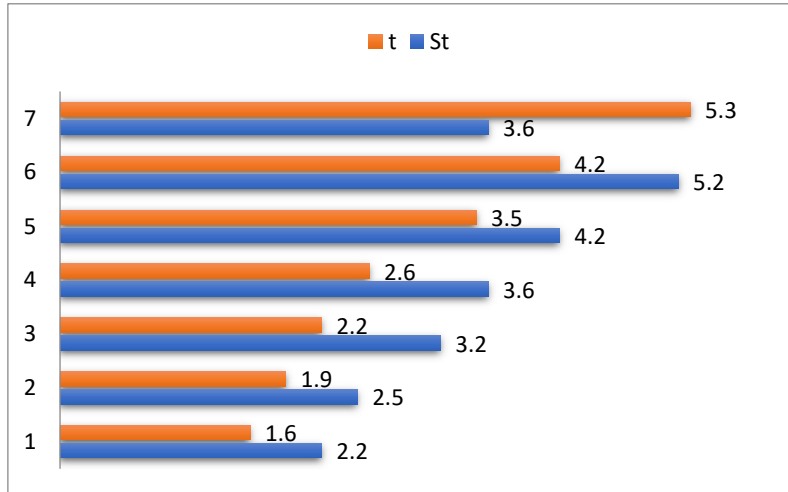


Figure 1: The baseband DME s' time area waveform

4. ENERGY DETECTION SPECTRUM SENSING MEETS ADAPTIVE

The range detecting issue might be treated as a paired speculation issue with two speculations H_0 and H_1 to address the nonattendance and presence of the DME signal in the channel, separately, within the sight of commotion and the OFDM signal.

Table 1: DME sign frequency domain waveform

Power (dB)	Frequency (MHz)
110	2.3
121	2.9
131	3.2
136	3.5
140	4.6
145	4.9
153	5.2

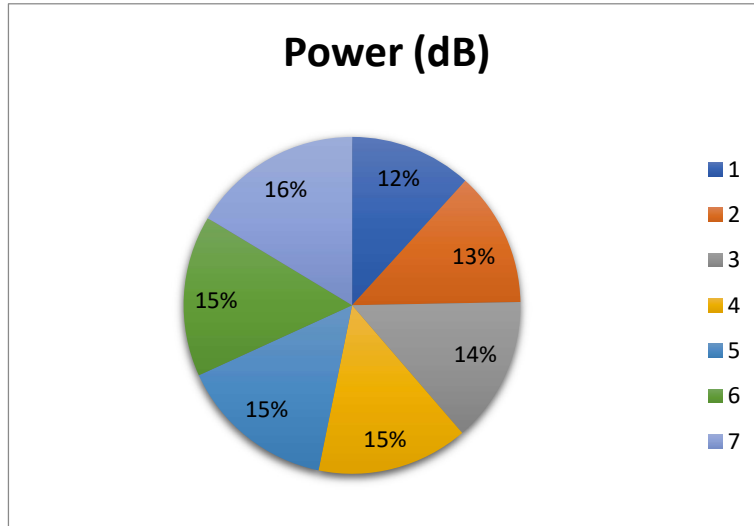


Figure 2: The DME sign's recurrence area waveform

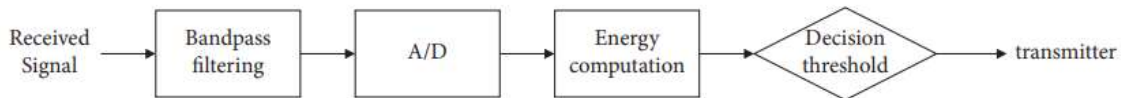


Figure 3: Versatile edge energy recognition model

DME and OFDM signals are sifted and isolated by their middle frequencies. The A/D transformer is then given the split DME sign and clamour. (R. Jain, 2011.) The accepted sign's energy is determined. In conclusion, the identifier picks the speculation and analyzes it to the limit. The discoveries are then sent back to the transmitter so range assets might be redistributed.

The following is the way the meaning of an identification measurement in different situations is determined:

$$T = \sum_{n=1}^N |y(n)|^2 \tag{3}$$

$$= \begin{cases} \sum_{n=1}^N |w(n)|^2, & H_0 \\ \sum_{n=1}^N |h * s(n) + w(n)|^2, & H_1 \end{cases}$$

Where N is the amount of sign examples got, 2s is the typical strength of the DME sign, and 2 represents commotion difference. (S. Kandeepan, 2019.) The conveyance of the test measurement under H0 and H1 might be given as follows founded on the CLT.

$$T \sim \begin{cases} N_c(N\sigma^2, 2N\sigma^4) & H_0 \\ N_c(N(\sigma^2 + \delta_s^2), 2N(\sigma^2 + \delta_s^2)^2) & H_1 \end{cases} \tag{4}$$

The increase of the channel might be expressed utilizing the following equation, where p alludes for the quantity of courses, and Nc(, 2) represents Gaussian appropriation with mean and difference 2.

$$\delta = \sum_{l=1}^p E[|h(l)|^2] \tag{5}$$

The likelihood thickness capability of T in two conditions might be derived from (8) as follows

$$f(T|H_0) = \left(\frac{1}{4\pi N \sigma^4}\right)^{1/2} \exp\left[-\frac{(T-N\sigma^2)^2}{4N\sigma^4}\right] \tag{6}$$

$$f(T|H_1) = \left(\frac{1}{4\pi N(\sigma^2 + \delta\sigma_s^2)^2}\right)^{1/2} \exp\left\{-\frac{T - N(\sigma^2 + \delta\sigma_s^2)^2}{4N(\sigma^2 + \delta\sigma_s^2)^2}\right\}$$

Thus, it is feasible to decide the probabilities of location, misleading problem, and missed caution.

$$p_d = P\{T > \lambda|H_1\} \tag{7}$$

$$= Q\left(\frac{\lambda - N(\sigma^2 + \delta\sigma_s^2)}{\sqrt{2N}(\sigma^2 + \delta\sigma_s^2)}\right)$$

$$p_f = P\{T > \lambda|H_0\}$$

$$= Q\left(\frac{\lambda - N\sigma^2}{\sqrt{2N}\sigma^2}\right)$$

where Q() is the right tail capability of the standard ordinary appropriation, now and again alluded to as the standard Gaussian reciprocal aggregate conveyance capability and is the versatile choice limit. Ordinarily, the limit is chosen to set Pf to a healthy level.

With a particular deception rate, the choice limit is given as

$$\lambda = \sigma^2 \left[\sqrt{2NQ^{-1}(P_f)} + N \right] \tag{8}$$

5. SIMULATIONS AND ANALYSIS

5.1. Simulation Setup

The recreation still up in the air by Tables 1 and 2, which are laid out as per the appropriate ICAO guidelines.

5.2 Results and analysis from simulations.

This part utilizes re-enactment utilizing MATLAB under different conditions to test the viability of the versatile edge energy identification approach in range detecting of the L-band DME signal. The complete number of discoveries for (e is arrived at the midpoint of more than 1000 acknowledge, and N 16200 examples are accessible for location.

SNR values for Re-enactments 1 are 20 dB, 18 dB, and - 15 dB. Figure 4 portrays a relationship diagram between the probability of discovery and the probability of a deception. As found in Figure 4, the adjustment of SNR affects discovery execution than the likelihood of deception. At the point when the SNR develops, the probability of discovery increments bit by bit. The opportunity of identification can increment to 100 percent at around Pf 0.05 with SNR 15 dB. In this way, the opportunity of location should increment to 100 percent at around Pf 0.35 with SNR 20 dB.

Re-enactments 2: To affirm the effect of an adjustment of SNR on location capacity, we chose the SNR range for perception to be between 20 dB and 5 dB. Figure 7 represents the effect of SNR for the versatile edge energy discovery procedure of the DME signal. The probability of recognition might move toward (. Shreejith, 2018.)100 percent when SNR is north of 12 dB, while location adequacy diminishes observably when SNR is below 12 dB. The location ability of Pf 0.1, nonetheless, is undeniably better than that of Pf 0.01 and Pf 0.05.

Table 2: LDACS signal

Items	Values
GHz carrier frequency	2
Transmission transfer speed/MHz	0.51256
Inspecting span/ μ s	2.7
Channel model	AWGN/multipath fading channel
Number of critical subcarriers	60
Adjustment mode	QPSK

Table 3: DME signal

Items	Values
Signal beginning time/ms	3
Transporter recurrence/GHz	1.3
Examining span/ μ s	2.7
Channel model	AWGN/multipath fading channel

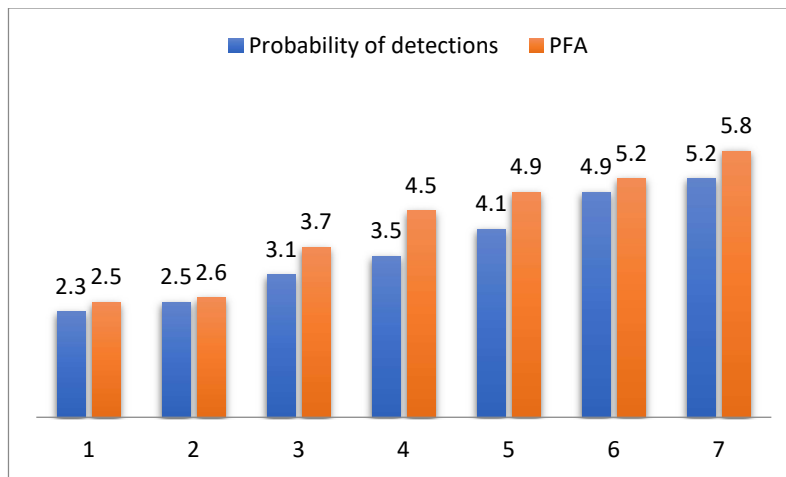


Figure 4: The relationship graph between the false alarm risk and detection risk at various SNRs.

Re-enactment 3: The strategy is reproduced under a similar likelihood of phony problem and SNR as the energy distinction identification technique (the energy contrast of the signs got in various channels is contrasted and the choice limit) to affirm the predominance of the versatile edge energy location technique for DME signal recognition.

Re-enactment 4: to confirm the practicability of the versatile edge recognition technique for the DME signal, the discovery cycle is recreated in multipath station and contrasted and the energy distinction identification strategy. Under the setting of reproduction 3, the quantity of

ways is 8, the Doppler recurrence shift is 1250 Hz, the postponement of every way is $\{0, 0.4, 0.8, 1.2, 1.6, 2.2, 2.4, \text{ and } 2.8\} \mu\text{s}$, and the power constriction of every way is $\{0, -1.7373, -3.4744, -5.2115, -6.9487, -8.6859, -10.4231, \text{ and } -12.1602\} \text{ dB}$.

6. CONCLUSION

It is encouraged to utilize LDACS, which works on the lower half of the L band as a trim framework between the two close by DME channels, as an expected decision for the future air-to-ground interchanges. By allowing dynamic range access (DSA) in the framework, the productivity of LDACS's range use might be expanded. In this review, a consistent misleading problem rate for the DME signal-based versatile edge energy location range detecting approach is proposed. (U. Epple and M. Schnell, 2011.) The essential client sign's past data, like the likelihood, signal strength, waveform, etc, are not needed by the (e technique in the message; DME is alluded to as the essential client). It offers highlights like a fast location time and a straightforward calculation. In this examination, we proposed a reconfigurable LDACS convention with a versatile casing structure and a reconfigurable sifted OFDM (Ref-OFDM) waveform that utilizes a low intricacy straight stage multi-band computerized channel. High out-of-band constriction grants more noteworthy transmission transfer speed as well as various narrowband transmissions, and the proposed convention and Ref-OFDM empower handsets to progressively change the transmission capacity across a wide reach to fulfil the expected nature of administration. The discoveries of the re-enactment show a significant improvement over the BER and no less than 32 dB less obstruction to existing L-band clients than the LDACS.

REFERENCES

1. D. Li, S. Li, and H. Liu, "Cyclostationary characteristics of carrier offset DME signals," *Systems Engineering and Electronic Technology*, vol. 38, no. 8, 2016.
2. E. Abd-Elaty, A. Zekry, S. El-Agoz, and A. M. Helaly, "Cognitive radio techniques for utilizing the primary L-band distance measuring equipment for aeronautical communications," *IEEE Access*, vol. 8, pp. 124812–124823, 2020.
3. J. Catherine and B. Sebastian, "A survey on DME interference mitigation techniques for L-band aeronautical communication," in *Proceedings of the 3rd International Conference on Computing and Communications Technologies*, pp. 253–257, Chennai, India, October 2019.
4. L. K. Mathew and A. P. Vinod, "An energy-difference detection based spectrum sensing technique for improving the spectral efficiency of LDACS1 in aeronautical communications," in *Proceedings of the 2016 IEEE/AIAA 35th Digital Avionics Systems Conference (DASC)*, pp. 1–5, Sacramento, CA, USA, September 2016.
5. L. K. Mathew, A. P. Vinod, and A. S. Madhukumar, "A cyclic prefix assisted spectrum sensing method for aeronautical communication systems," in *Proceedings of the 2019 IEEE International Symposium on Circuits and Systems (ISCAS)*, pp. 1–5, Sapporo, Japan, May 2019.
6. M. Mostafa, N. Franzen, and M. Schnell, "Dme signal power from inlay LDACS1 perspective," in *Proceedings of the 33rd Digital Avionics Systems Conference*, Colorado Springs, CO, USA, October 2014.
7. M. Sajatovic, B. Haindl, M. Ehammer et al., *LDACS1 System Definition Proposal: Deliverable D2, Eurocontrol Study, Brussels, Belgium, 2009.*

8. M. Schnell, U. Epple, D. Shutin, and N. Schneckenburger, "LDACS: future aeronautical communications for air-traffic management," *IEEE Communications Magazine*, vol. 52, no. 5, pp. 104–110, 2014.
9. M. Schnell, U. Epple, N. Fistas, and EUROCONTROL L-DACCS2, *System definition proposal: deliverable D2, European air traffic management, Brussels, Belgium, 2009.*
10. M. Schnell, U. Epple, S. Brandes, and EUROCONTROL L-DACCS1, *System definition proposal: deliverable D3-specifications for L-DACCS1 prototype, European air traffic management, Brussels, Belgium, 2009.*
11. N. Neji, T. Letertre, O. Outtier, R. de Lacerda, and A. Azoulay, "Survey on the future aeronautical communication system and its development for continental communications," *IEEE Transactions on Vehicular Technology*, vol. 62, no. 1, pp. 182–191, 2013.
12. R. Jain, F. Templin, and K. S. Yin, "Analysis of L-band digital aeronautical communication systems: L-DACCS1 and L-DACCS2," in *Proceedings of the IEEE 2011 Aerospace Conference*, pp. 1–10, Big Sky, MT, USA, March 2011.
13. S. Kandeepan, *Cognitive radio technology - spectrum sensing, interference mitigation and location*, National Defense Industry Press, Beijing, China, 2019.
14. S. Shreejith, L. K. Mathew, V. A. Prasad, and S. A. Fahmy, "Efficient spectrum sensing for aeronautical LDACS using low-power correlators," *IEEE Transactions on Very Large Scale Integration Systems*, vol. 26, no. 6, pp. 1183–1191, 2018.
15. U. Epple and M. Schnell, "Overview of interference situation and mitigation techniques for LDACS1," in *Proceedings of the 2011 IEEE/AIAA 30th Digital Avionics Systems Conference*, pp. 4C5-1–4C5, Seattle, WA, USA, October 2011.